In: AIAA SCITECH 2025 Forum, 6-10 January 2025, Orlando, FL, UAS. Paper number AIAA 2025-2680
DOI:10.2514/6.2025-2680

Single- and Two-Stage Fan Designs for a Supersonic Airliner with Focus on Certification Noise Reduction

Matti Graebert[1], Robert Jaron[1], Cristina Villena Munoz[2], Martin Plohr[3], and Antoine Moreau[1]
[1]*German Aerospace Center (DLR), Department of Engine Acoustics, Bismarckstr. 101, 10623 Berlin, Germany*
[2]*Cranfield University, Department of Aerospace Engineering, College Road, Cranfield MK43 0AL, UK*
[3]*German Aerospace Center (DLR), Engine Department, Linder Höhe, 51147 Cologne, Germany*

A comprehensive analytical approach is taken to compare the aerodynamic performance as well as the landing and take-off noise of a single and a two-stage fan at pre-design level. The fans were designed for the engines of a supersonic airliner with the goal of minimizing noise certification levels. The prediction of aerodynamic performance is performed for on- and off-design points using analytical and semi-empirical models, the noise for landing and take-off operations is calculated using analytical approaches in modelling noise sources and propagation to the certification points. Certification metrics are also calculated and used in this comparison. This process is run for both fan designs on a baseline take-off trajectory in accordance with current regulations, as well as an optimized trajectory exploiting potential regulation changes for supersonic aircraft. With this study, the authors are able to demonstrate that a two-stage fan design produces significantly lower noise levels. In configurations and on trajectories on which fan noise is dominant, significantly lower certification levels could be achieved.

Nomenclature

Acronyms

BBN	Broadband noise
LTO	Landing and take-off
R	Rotor
S	Stator
SST	Supersonic Transport
TE	Trailing edge (noise)
ToC	Top of climb
$VIGV$	Variable inlet guide vane
$VNRS$	Variable noise reduction system
VTN	Variable throat nozzle

Variables

η	Efficiency
ϕ	Flow coefficient
Ψ	Pressure range
BPR	Bypass ratio
d	Diameter, m
$EPNL$	Effective perceived noise level, $EPNdB$
FPR	Fan pressure ratio
l	Length, m
M	Mach number

Published by AIAA. This is the Author Accepted Manuscript issued with: Creative Commons Attribution License (CC:BY 4.0).
The final published version (version of record) is available online at DOI:10.2514/6.2025-2680. Please refer to any applicable publisher terms of use.

$MTOM$	Maximum take-off mass, kg
PLR	Programmed lapse rate
PNL	Perceived noise level, dB
$PNLT$	Tone-corrected perceived noise level, dB
SPL	Sound pressure level, dB
t	Time, s
TKE	Turbulent kinetic energy, $m^2 s^{-2}$
V	(Air) Speed, m/s, kts

I. Introduction

More than 20 years have passed since the last civil supersonic flight but the development of the next generation of such aircraft is well underway. With a projected market entry as soon as 2030 [1], there is a need for environmental regulation of supersonic transport (SST). The data, which regulators require to draft appropriate certification rules for supersonic aircraft, is provided by companies designing those new aircraft but also independent researchers, for example in the EU project SENECA. Within SENECA, the environmental impact of SST is investigated. For that purpose, four aircraft are designed: two supersonic business jets with respective cruise speeds of Mach 1.4 and 1.6 and two supersonic airliners with respective cruise speeds of Mach 1.8 and 2.2. Their landing and take-off noise and en-route emissions are modelled and the scaled according to market studies.

This paper will focus on the landing and take-off noise which are essential to the certification of new aircraft. Only engine noise will be considered, because it is the dominant noise source during take-off [2] and also significant or dominant during landing. Since the focus of this paper is the comparison of fan designs, fan noise will be investigated first and foremost. Jet noise will be included in all calculations since it is the other significant, potentially dominant contributor to engine noise of supersonic aircraft.

Those engines are significantly different to subsonic aircraft engines. They are usually low- to mid-bypass turbo engines instead of modern high-bypass designs due to the high drag larger nacelles incur at high speeds. The inlets of supersonic aircraft are more complex than those of subsonic aircraft. They must create effective shock systems for compression in supersonic flight. Furthermore, the high thrust required in cruise and low thrust on approach dictate a very wide range of operations for such engines, often necessitating the use of variable features such as variable inlet guide vanes (VIGVs) or a variable throat nozzle (VTN). The design point for supersonic aircraft engines is the Top of Climb (ToC) because it is the most critical point in thermal management due to the high altitude and thrust requirement. It also marks the beginning of the cruise, so it is representative of the cruise operating conditions. To provide sufficient thrust, especially at high cruising speeds, the fan pressure ratios (FPR) are much higher than that of subsonic aircraft engine fans at around 2.0. In order to achieve such high FPRs, a single fan stage has to be highly loaded and run at very high transonic speeds. To maintain flow stability, the high stage loading requires the rotor to be a wide-chord design. Alternatively, a two-stage fan design can distribute the pressure increase over its two stages, reducing the required fan speed and aerodynamic loading, which allows more slender blades. Fan speed and stage loading are significant for fan noise generation, so this design choice has an impact on supersonic aircraft landing and take-off (LTO) noise and thus the critical certification noise levels. In this paper, one single stage and one two-stage fan design will be introduced and their impact on certification noise levels explored. The fan and jet noise of the engines of a supersonic airliner as well as the noise propagation to observers on the ground are modelled using analytical and empirical models, on one approach and two take-off trajectories.

The fans analyzed in this paper were designed for an engine powering a supersonic quadjet concept with a cruise Mach number of 1.8 and a capacity of 100 passengers [3]. At the design point, ToC, the engine has a bypass ratio $BPR = 2.67$ and a fan pressure ratio $FPR = 2.09$ [4].

A. Structure of the paper

To compare the certification noise levels of a single- and two-stage fan design, two fans have to be designed, their noise sources simulated and propagated to noise certification points and finally the resulting EPNdB have to be calculated. To comprehensively cover this process, first an overview of the current state of research on the topic of

supersonic aircraft landing and take-off noise is presented below. The aerodynamic and acoustic methods used in this study will be explained in Section II. After a cursory explanation of the aircraft and engines for which the fans are designed in Section III, the fan designs are introduced in the ensuing section (IV). As the final input into the calculations, the flight profiles are discussed in Section V). Then the results will be shown, analyzed and discussed in Section VI: certification noise levels of both fan designs for a baseline and an optimized flight profile. Finally, the conclusions are drawn from those results.

B. Current state of research

Since the engines of civil supersonic aircraft are either built as prototypes or at even earlier steps in development, measurements of their noise levels are not available and methods of noise prediction need to be relied on. Only data from the earliest stages of this development are publicly available, so the study will have to be conducted on a pre-design level.

Several empirical models for fan noise prediction such as the Heidmann model [5] and its derivatives [6, 7] have been calibrated using single stage fans and are widely used. Gliebe developed another empirical model which was calibrated using a two-stage fan [8] within the High Speed Research (HSR) Program which is published in the *HSRNOISE* software tool's manual [9]. It does however only simulate noise radiated upstream of the flow originating in the first stage. These empirical models have been used in the past to predict SST certification noise [2, 10–13], mostly with the goal of optimizing take-off trajectories.

Their use in predicting the noise of a multi-stage SST fan with a high FPR is limited. Stephens [14] was able to demonstrate that the Gliebe model can predict the EPNL metric of a single fan with an accuracy of 0-3dB (depending on the fan speed), however the directivity prediction is shown to be unreliable. The fan of the XF-120 engine used for those measurements was developed in the 1980s for a military application and cannot be assumed to be a modern civil design, with the engine having a BPR of 0.32. Specific design data is not publicly available due to the confident nature of military technology. the confidential. Empirical models do not model the physical noise generation mechanisms and do not further the understanding of them. For that reason, their usefulness for the design process is limited as well.

Numerical and analytical models offer an alternative [15, 16] and can be used in SST trajectory optimization studies [17]. They offer their own advantages and disadvantages: while the absolute noise levels are less accurate with analytical models, they show trends and physical mechanisms behind the noise sources reliably [18]. Analytical models can be operated at much lower computational cost than numerical methods, which allows larger parameter studies. For more accurate noise prediction, numerical methods are preferable. While their results are very reliable, their computational cost is very high.

Civil research on multi-stage fans was conducted as early as the 1970s, for example by NASA [19–21]. With higher bypass ratio engines and decreasing FPRs, the interest in civil multi-stage fans decreased as well. Early noise studies already focused on high BPR single stage fans [22]. For military applications, multi-stage fans kept being developed and can produce FPRs of 2.5 to 5 [23].

While there are many LTO noise studies for SST, they employ empirical noise models and do not evaluate detailed fan designs and their impact on LTO and certification noise levels. Physics-based models allow a deeper understanding of the operation of single and especially multi-stage fans and their noise emissions. They will be used to evaluate a noise optimized single and two-stage fan design with regards to their impact on SST certification noise.

II. Methods

In this section the methods for predicting the fan aerodynamics and source noise levels, modelling noise propagation and calculating noise certification levels are introduced and their application in designing the one- and two-stage fans explained.

A. Determining noise certification levels

In order to determine an aircraft's noise certification levels, flyover noise measurements at three distinct positions are conducted (as in Fig.1):

- Approach: On centerline, 2000 m before the runway threshold
- Lateral: 450 m laterally removed from the centerline, at the longitudinal position where the highest sound pressure level (SPL) is recorded
- Flyover: On centerline, 6500 m from brake release.

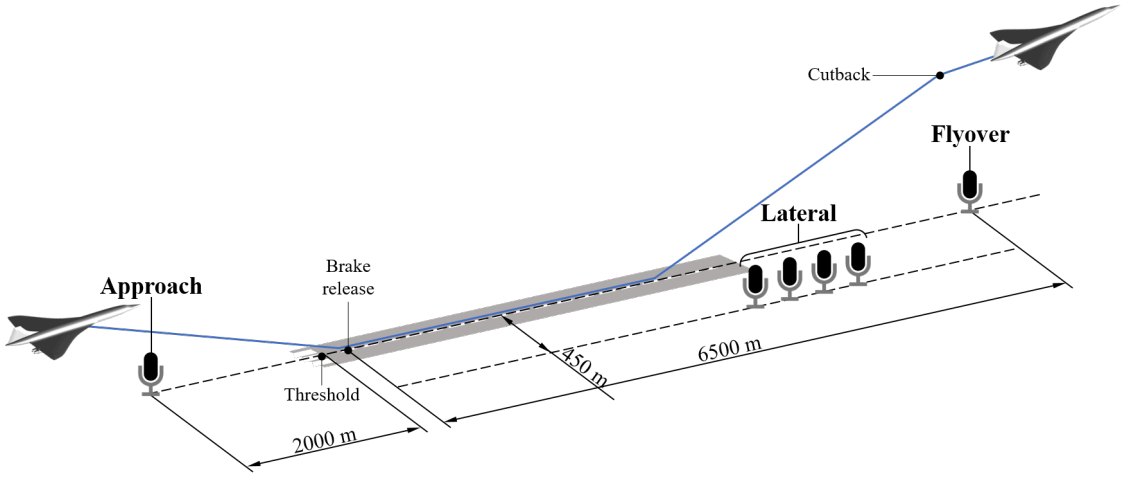

Fig. 1 Location of certification measurement points along flight profile

Each microphone is positioned 1.2 m above the ground. The SPL is measured every 0.5 s during the flyover. By weighing depending on its frequencies, the SPL are then converted to the perceived noise level (PNL). Tone-corrected perceived noise levels (PNLT) are calculated by applying a penalty for tones. The goal is to adjust the physical sound metric SPL for annoyance to the observer. The peak of PNLT over time has to be determined and a time window $[t_1, t_2]$ found, where t_1 marks the first time step at which the PNLT is less than 10 dB below the peak value and t_2 the last time step at which this is the case. The EPNL is then calculated by integrating the PNLT between t_1 and t_2.

For noise prediction, the process chain needs to altered since no measurements can be made. The general three step approach taken in this paper is shown in Fig.2

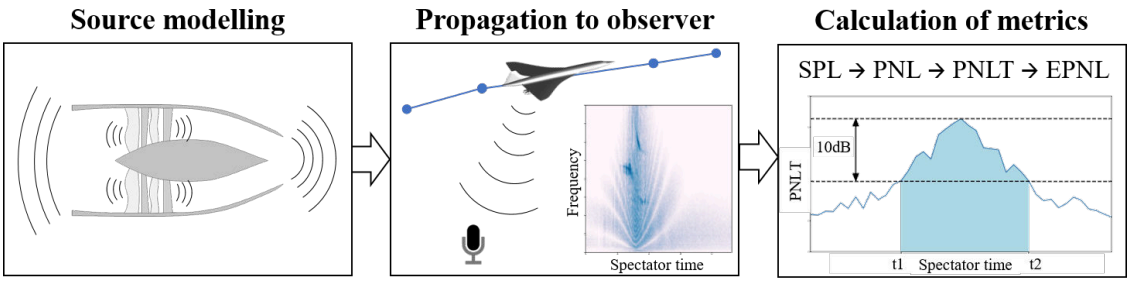

Fig. 2 General approach to predicting noise certification levels

B. Analytical modelling of fan aerodynamics and noise sources

The DLR in-house tool *PropNoise* is used for predicting the fan aerodynamics and noise levels at source as well as propagating them to the near-field. It is a framework based on semi-analytic models that relies on the idea that simplified, physics-based methods can help to improve understanding turbofan engines, which are very complex systems and provide guidelines for noise reduction. Since a design-to-noise approach necessitates considering both engine performance and noise emission, the appropriate thermodynamic, aerodynamic and acoustic models are coupled in the same framework. The general structure and approaches of *PropNoise* are described by Moreau [24]. For the sake of brevity, it will not be elaborated on further in this paper. The most significant simplifications for supersonic aircraft fans in the modelling of noise sources and propagation to the near-field are:

- The inlet is assumed to be a circular duct
- Transmission effects of noise passing through fan stages (scattering, transonic rotor shielding) are ignored

Buzzsaw noise is usually the dominant noise source in transonic fans. To describe the pressure signature upstream of a transonic rotor, comprising both potential field and shocks, an analytical model was developed by Moreau [25].

It models both shock generation, propagation and decay. Strip theory is employed, so the strips are calculated as independent 2D problems. A purely axial inflow and uniform background flow are assumed, so scattering due to inflow distortion is neglected. The model can predict shock systems for ideal and non-ideal blades. In this study, the blade angles are assumed to be non-ideal with a random distribution of angle deviations within an interval of $[-0.4, 0, 4]$ degrees. This leads to the excitation of more modes and a more realistic buzzsaw noise signal.

The jet is assumed to be a perfectly mixed single stream and will thus be modeled using the empirical Stone jet noise model of 1983[26].

The sources are considered in this paper can be found in Table 1. Some of them will be used in abbreviated form throughout the rest of the paper.

Source	Type	Abbreviation
Rotor-Stator Wake Interaction	Broadband + Tonal	Wake R-S/S-R
Rotor-Stator Potential Field Interaction	Tonal	-
Trailing Edge	Broadband	TE R/S
Buzzsaw	Tonal	-
Jet	Broadband	-

Table 1 Modelled engine noise sources

C. Modelling of noise propagation to observer

To realistically model the propagation of noise from an aircraft engine moving along a designated trajectory with varying operating points to an observer in the far-field, a framework of analytical and empirical models was developed. This framework is implemented as the DLR in-house tool $VIOLIN$. The analytical methods and approaches to propagate the engine noise to an observer are detailed by Moreau et al [27]. The propagation effects included in the modelling are:

Effect	Modelling approach
Spreading loss	-
Doppler effect	-
Atmospheric attenuation	According to ISO 9613-1 [28]
Ground attenuation	SAE AIR 6552 [29]
Atmospheric jitter	Enhanced Rietdijk Method [30]

Table 2 Modelled propagation effects

D. Liner attenuation

Since fan noise proved to be the dominant noise source without additional attenuation (see VII), it is of high importance to model liner attenuation. For current subsonic aircraft engines liner play a major role in reducing fan noise. Their impact can be expected to be much more significant for supersonic aircraft engines: the geometry with long inlets and bypasses allows for a high liner length, especially in relation to the small diameters. The small diameter also dictates higher rotational speeds, causing higher frequency tones which can be attenuated more easily even with shallow liners.

However, developing a liner for this application or tuning a common liner model is outside the scope of this paper. This is why a simplified approach is chosen which assumes a perfectly tuned liner with the following properties:

- A flat rate noise attenuation over all frequencies depending on whether they are tonal or broadband sources
- The liner attenuation scales linearly with liner length, neglecting effects of decreasing liner efficiency with increasing liner length
- The liner is designed for take-off and will work with 100% effectiveness in any take-off setting; for the lower fan speeds on approach, the effectiveness is 70%

- Since discrete frequencies can be dampened with liners much more efficiently, the liners are capable of attenuating broadband sources by -10 dB per l/d (where l is the liner length and d is the duct diameter) and tonal sources by -20 dB per l/d

The flat rate attenuation entails the assumption that no non-dominant tone emerges as dominant due to dampening of previously dominant tones. The estimated attenuation is loosely based on papers by Rice [31–34] who studied the large-scale impact of liners. Small studies with an extended Helmholtz resonator model [35] indicate that they are a rough match with peak attenuation of Helmholtz resonators.

With relative lengths of inlet being $\frac{l_{inlet}}{d_{inlet}} = 1.5$ and of the bypass being $\frac{l_{bypass}}{d_{bypass}} = 6.0$, the total attenuation is assumed to be:

	Inlet Take-Off	**Bypass Take-Off**		**Inlet Approach**	**Bypass Approach**
Broadband attenuation [dB]	-15	-60		-10.5	-42
Tonal attenuation [dB]	-30	-120		-21	-84

Table 3 Assumed liner attenuation

The authors of this paper feel that it is a strong assumption, but an improvement over excluding liner effects entirely. The results without liners can be found in the appendix.

III. Aircraft and Engines

The aircraft used for this study, including airframes and engines, are conceptual designs at a pre-design level. The platform is defined to be representative passenger aircraft cruising at M=1.8. The main design parameters are listed in Table. 4. Further details on aircraft design and specifications are given by Munoz et al. [3].

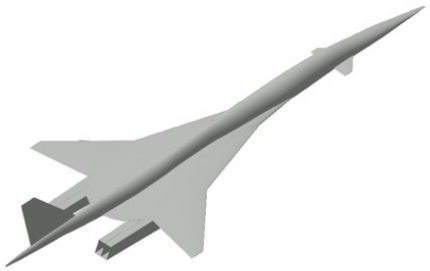

Cruise Mach number	1.8
Passengers	100
Range [nm]	4000
MTOM [t]	144.3
Number of engines	4
Wing area [m^2]	427.3
Wing loading [kg/m^2]	337.7
Overall length [m]	71.6
Span [m]	35.0

Table 4 Platform specifications

The engines for this platform were designed and optimized for efficiency and thrust demand of the overall flight mission profiles while not jeopardizing the LTO noise certification limits. These are conflicting design goals, because cruise efficiency increases with a low BPR and small engine diameter. This also increases the jet velocity during operation which is a significant driver of engine noise. This engine was designed by German Aerospace Center (DLR) [4]. Only current technologies with a potential entry into service 2025 to 2035 were considered. Relevant parameters of these engines can be found in Table 5.

The variable throat nozzle in the engines allows to regulate the mass flow and jet velocity. In order to reduce jet velocities and thus jet noise, they are set to be fully opened for all LTO operations. This greatly increases the mass flow and moves all LTO operating points to the lower right end of the fan map (high mass flow, low FPR). These operating points are close to, or in some cases, in choking conditions.

Engine Architecture	2-stage fan, variable throat nozzle
Net thrust per engine [kN]	133
TSFC [g/kNs]	17.1
Fan diameter [m]	1.64
Bypass ratio	3.19
Fan pressure ratio	1.94
OPR	21.9

Table 5 Engine specifications at sea level, EOF ISA+15K with M=0.25

IV. Fan designs

In this section, the fan designs which are compared will be presented. Both fans have been designed using the methods described by Graebert et al [36] with a focus on aeroacoustic optimization along with aerodynamic properties: first, a fan is designed using general design rules, then the fan design gets optimized by an evolutionary algorithm. This algorithm weighs aerodynamic performance at ToC and acoustic properties in LTO operations and iterated parameters such as blade numbers within a predetermined design space. After convergence, this results in a quiet fan design with high cruise efficiency, with stable operation in the relevant operating points.

The geometric parameters of both fans are displayed in Tables 6 and 7, the performance parameters in Table 8. A simplified meridional view of the designs is displayed in Fig. 3. The rotor sections are strongly converging to stabilize the flow in cruise and other high power settings. The duct directly upstream of the (second stage) stator is divergent to reduce the axial flow speed in low power settings with small stage pressure ratios and avoid choking the stator.

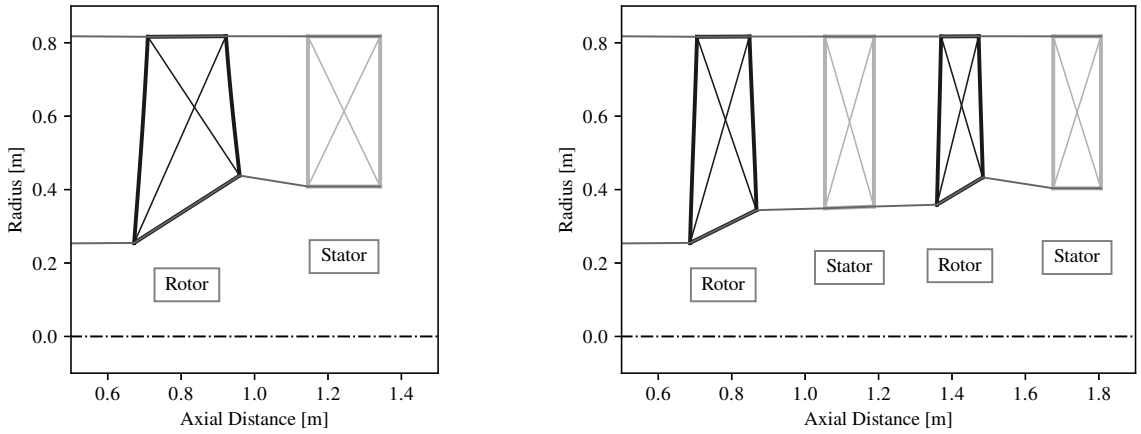

(a) Single stage fan **(b) Two-stage fan**

Fig. 3 Single stage (left) and two-stage (right) fan schematics in meridional view

Rotor chord [m]	0.406
Total bladed length [m]	0.642
Rotor blade number [−]	16
Stator blade number [−]	47
Rotor solidity [−]	1.53
Stator solidity [−]	2.33
Rotor MDVR [−]	1.26
Stator MDVR [−]	1.03

Table 6 Single stage fan geometry parameters

Rotor-1 chord [m]	0.230
Rotor-2 chord [m]	0.178
Total bladed length [m]	0.985
Rotor-1 blade number [−]	19
Stator-1 blade number [−]	37
Rotor-2 blade number [−]	29
Stator-2 blade number [−]	57
Rotor-1 solidity [−]	1.06
Stator-1 solidity [−]	1.23
Rotor-2 solidity [−]	1.18
Stator-2 solidity [−]	1.84
Rotor-1 MDVR [−]	1.10
Stator-1 MDVR [−]	1.01
Rotor-2 MDVR [−]	1.12
Stator-2 MDVR [−]	1.02

Table 7 Two-stage fan geometry parameters

	Single Stage	**Two-Stage**
FPR	2.09	2.09
Relative tip Mach number	1.61	1.28
η_{ise}	0.891	0.922
ϕ	0.53	0.73 | 0.55
Ψ	0.99	0.83 | 0.84

Table 8 Aerodynamic parameters of both fans at ToC

The different advantages of each design can clearly be seen: due to the lower stage pressure ratio and lower stage ratio pressure range Ψ, the two-stage fan can run at much lower speeds and thus higher efficiency η_{ise} than the single stage design (see Table 8). The negative correlation between stage pressure ratios bigger than 1.2 and isentropic efficiency was already demonstrated by Moreau [24], the reduction in efficiency with increasing tip Mach numbers of high speed rotors due to shock losses by Miller et al [37]. The chord length of the two-stage rotors is significantly smaller than the single stage rotor, due to the lower pressure range Ψ, which is the total isentropic enthalpy difference normalized with the square of the rotational speed. The single stage fan on the other hand is shorter in total bladed length, simpler and most likely substantially lighter. However, these comparisons are not within the scope of this paper. It will focus on their acoustic properties in LTO operation.

V. Trajectories

The trajectories explored in this paper are simplified 2D flight profiles. They abide the ICAO regulations but are not adjusted to the take-off procedures of individual airports. Since they are made up of concrete points, step-wise changes to corresponding engine parameters and interpolation artifacts are present within the data.

The maximum thrust requirement for subsonic aircraft is at take-off, so the engine is designed to provide this thrust with a safety margin. Supersonic aircraft require a very high thrust to maintain their supersonic cruise speed at altitude. For this reason, the engines can produce a large surplus of power at low altitude and speeds. This allows for a strong de-rate at take-off. Since LTO noise is a significant limit to the operation of civil SST, variable noise reduction systems (VNRS) were proposed to make use of this characteristic. VNRS is permanent onboard equipment which automatically changes the operating condition or configuration of the aircraft without manual activation by the flight crew to reduce noise. This broad definition can encompass many different systems which can be used to alter the take-off and landing procedures.

The changes to the take-off procedure used in the optimized trajectory for this paper are:

- Programmed Lapse Rate (PLR): The automatic reduction in thrust to a predefined level at a predefined height
- Fast Climb-Out: Increased speed during climb, currently limited to $V_2 + 20kts$
- De-rated Take-Off: Reduction in the take-off thrust (from beginning of take-off roll)
- Delayed Rotation: Delaying the lift-off after reaching rotation speed V_R in order to build up more speed while on the ground

All these adjustments serve to reduce the thrust requirements during take-off by taking advantage of the increasing aerodynamic efficiency of supersonic aircraft with higher speeds or reducing the applied thrust to the lowest safe level. Since engine noise has a strong correlation to thrust all these changes will reduce engine and thus LTO noise significantly.

A. Baseline trajectory

The baseline trajectory was calculated using the maximum take-off thrust with an open nozzle, guaranteeing a subsonic jet. No variable noise reduction systems (VNRS) are considered and the climb-out speed it set at $V2 + 20kts$, the maximum allowed by current regulations. No pilot activated cutback is conducted and the climb performance maximized at all times.

B. Optimized trajectory

To find the trajectory with the lowest cumulative EPNL while not violating the limits at the individual certification points, a trajectory variation study was run with the following constraints:

- Maximum field length: $10.000ft$
- Cutback at $20.000ft$ vertical distance from break release
- Minimum cutback height: $689ft$ as per regulations for four engine aircraft
- Minimum climb angle at all times: $4\%(\approx 2.3°)$ as per regulations [38]

In a trajectory variation study, the VNRS parameters explained above were varied to form a 5-dimensional matrix using the same aircraft and engine [17]. The trajectory with the highest cumulative margin to Chapter 14 noise limits was found. The parameters of this optimized trajectory as well as the baseline trajectory are listed in Table 9.

	Baseline	Optimum
PLR Level [%]	100	70
PLR Activation Height [ft]	-	35
Climb-Out Speed V2+X [kts]	20	72
Take-Off De-rate [%]	80	60
Delayed Rotation [kts]	161	221

Table 9 Trajectory variations and optimum trajectory

The altitude, thrust and speed profiles can be seen in Fig.4.

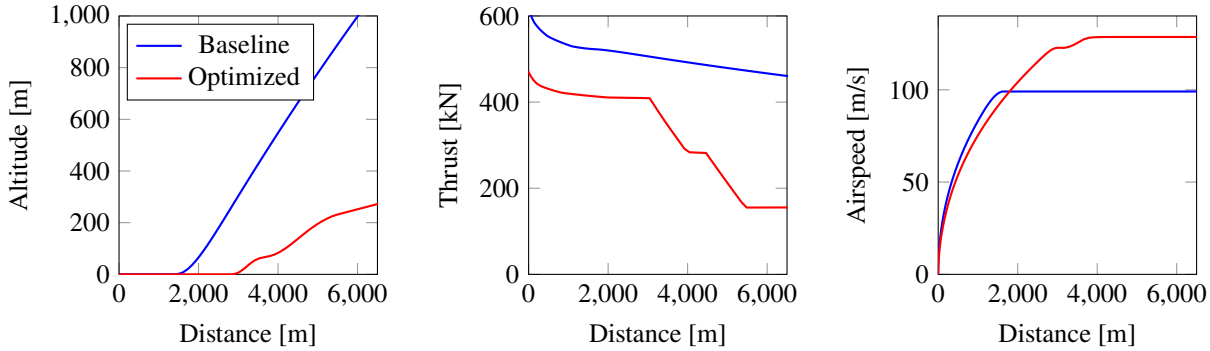

Fig. 4 Parameters of baseline and optimized take-off trajectories

C. Approach

The approach is performed with a standard 3° glideslope. The operating point of the engine can be considered stationary for the approach, since a change in thrust demand, aircraft attitude or airspeed only occurs a long distance before and after the noise certification point.

The relevant flight parameters at the approach certification point are:

- Altitude: 120m
- Thrust: 73.7 kN
- Airspeed: 70.1 m/s

VI. Results

This section discusses the results of the noise certification level predictions. First the levels for the Approach point are compared, using a representative landing trajectory. Then the two take-off certification points Lateral and Flyover are considered, on both the baseline and optimized take-off trajectory. The fan maps of both designs are shown in Fig.5, along with the operating points discussed in this section. The operating points for baseline lateral and flyover certification point are so close that they are not listed and plotted separately.

Both fans have similar maps and the design goal of covering the mission envelope is met. All LTO operating points except for the baseline operation (point 5) are at low thrust settings. It is clear to see that the open nozzle moves the operating points towards choking conditions, or in the case of the high thrust baseline operation, into choking. The operating conditions for each representative point will be shown when their noise results are discussed. Especially at low power settings, such as Approach (point 1), the two-stage fan as a much wider operating range between choking and surge line.

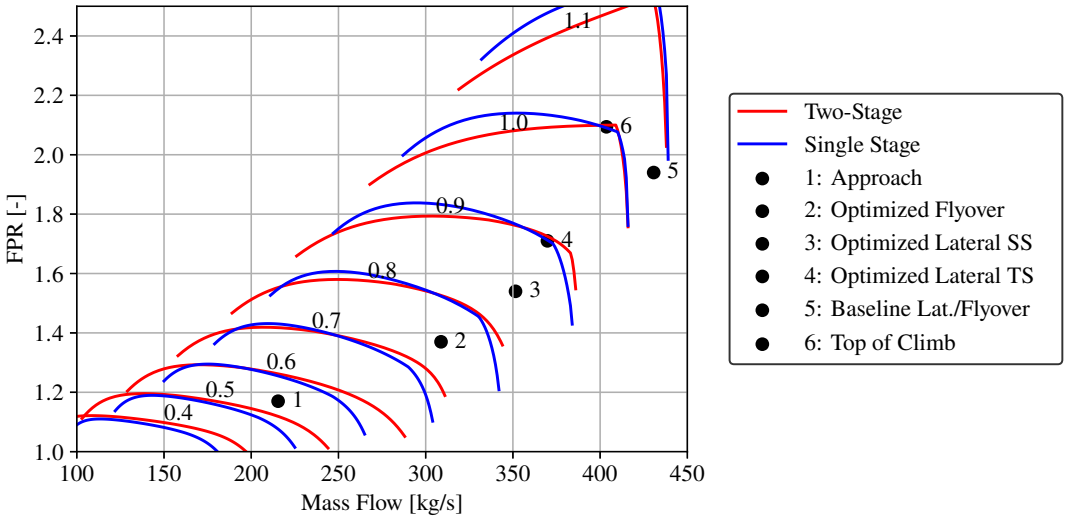

Fig. 5 Fan maps with relevant operating points with relative fan speed on respective throttle lines; SS denotes the single stage and TS the two-stage design

A. Approach

Due to the nature of an idealized glideslope approach, operating point on approach is quasi-static. The parameters relevant to noise in Approach configuration can be found in table 10. These parameters were calculated using the aerodynamic and thermodynamic models of *PropNoise*. The jet Mach number is relevant for jet noise, the rotor relative tip Mach number for buzzsaw and incidence as well as wake parameter for wake interaction noise. The liner effectiveness for this operating point is assumed to be 70%, so fan noise is not attenuated as effectively as on take-off.

	Single Stage	**Two-Stage**
Rel. Thrust [%]	14.4	
FPR [–]	1.17	
Jet Mach Number [–]	0.45	
Rel. Fan Speed [%]	50.9	52.0
Front Rotor Rel. Tip Mach Number [–]	0.82	0.64
Front Rotor Incidence [°]	6.3	7.1
Front Rotor Wake Area [–]	0.063	0.047
Front Rotor Mean Wake TKE [m^2/s^2]	161.7	67.1

Table 10 Approach operating point parameters

The temporal variation of the PNLT as well as both fan and jet noise at the approach microphone can be seen in Fig.6. In the graph, the 10 dB down time for each fan design is marked in the respective colors (blue and red), with overlapping intervals in purple.

The fan noise of both designs is dominant over the jet noise and the two-stage design produces lower noise levels than the single stage design. Fig.7 shows the temporal variation of all relevant sources for both fans, which helps explain the difference in fan noise between the two designs.

		Approach
Single Stage	**Limit**	101.8
	Noise Level	87.9
	Margin	13.9
Two-Stage	**Noise Level**	80.2
	Margin	21.6

Table 11 Approach noise certification levels in EPNdB

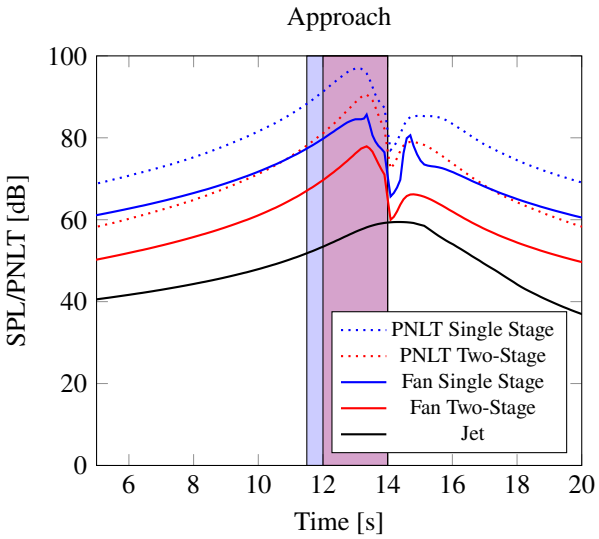

Fig. 6 SPL on Approach, with 10dB down time

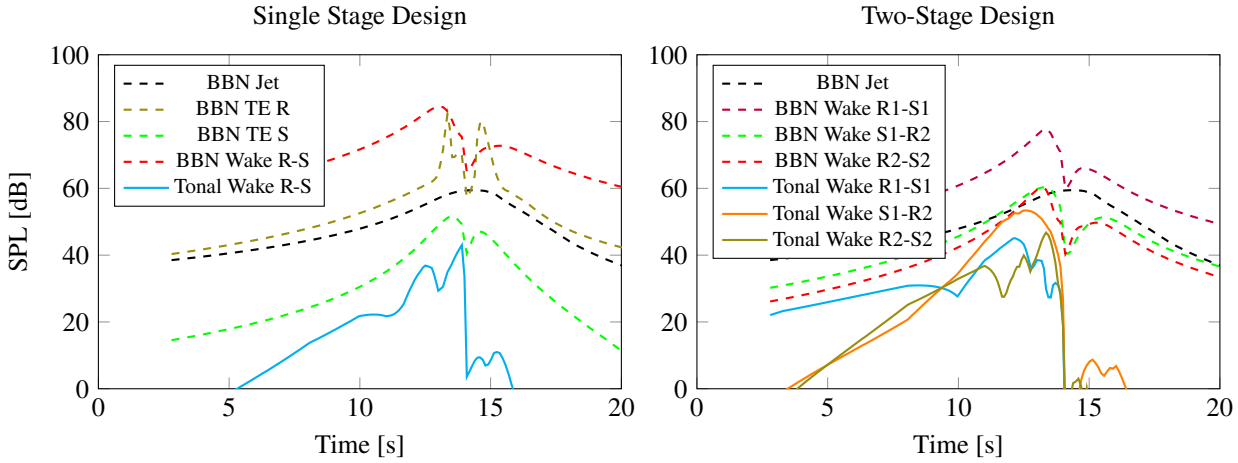

Fig. 7 Individual noise sources at Approach microphone, broadband sources with dashed and tonal sources with solid plots

Since the engine operates at only 14.4% of the maximum LTO thrust, relative fan speeds of 52% or lower in approach, neither jet nor buzzsaw are dominant noise sources, with a low jet and subsonic relative tip Mach number (see Table 10). The dominant noise source in the 10dB down time, where the PNLT peaks, is the broadband wake interaction noise between (first stage) rotor and stator. This is due to the operation in far off-design conditions, which results in large rotor incidences and consequently, large wakes with strong turbulence. These wakes cause strong broadband rotor-stator interaction noise for both fan designs. The larger chord of the single stage fan rotor compounds this problem, as can be seen in the wake area, the product of wake width and wake deficit speed normalized with mean flow speed and turbulent kinetic energy (TKE) in Table 10. This is the reason the single stage design is significantly louder than the two-stage design, with larger, more turbulent wakes. Transonic rotor shielding does not occur in this case since the rotors of both fans are subsonic across their entire span.

The resulting Approach certification point noise levels for both fan designs can be seen in Table 11. These margins are very high and considered unrealistic by the authors. Possible reasons for this are discussed at the end of this section.

B. Take-Off on Baseline Trajectory

On the baseline trajectory, the power setting is set to the maximum the engine can provide with a fully open nozzle. This leads to the fan temporarily operating very close to the choking line and outside of ideal operating conditions. The operating point at the moment when the plane is at minimum distance to the microphone will be considered the most representative for each certification point. The relevant engine parameters of these operating points can be found in Table 12.

	Single Stage	**Two-Stage**
Rel. Thrust - Lateral [%]	100.0	
FPR - Lateral [–]	1.94	
Jet Mach Number - Lateral [–]	1.02	
Rel. Fan Speed - Lateral [%]	105.6	106.2
Rel. Tip Mach Number - Lateral [–]	1.84	1.47
Rel. Thrust - Flyover [%]	100.0	
FPR - Flyover [–]	1.94	
Jet Mach Number - Flyover [–]	1.01	
Rel. Fan Speed - Flyover [%]	105.6	106.2
Rel. Tip Mach Number - Flyover [–]	1.86	1.48

Table 12 Parameters of baseline take-off operating points

Due to the high power setting and fan pressure ratio, the jet velocity is so high that jet noise becomes the dominant noise source, as can be seen in Fig.8. Despite it being a broadband, low frequency source, it dominates the PNLT at the time of the fly-by. For this reason, the fan noise has no significant impact on the take-off certification noise. The sudden drop in all fan noise at the moment of the fly-by is due to the very strong downstream liner attenuation. The take-off certification noise levels on the baseline trajectory for both fan designs can be seen in Table 13.

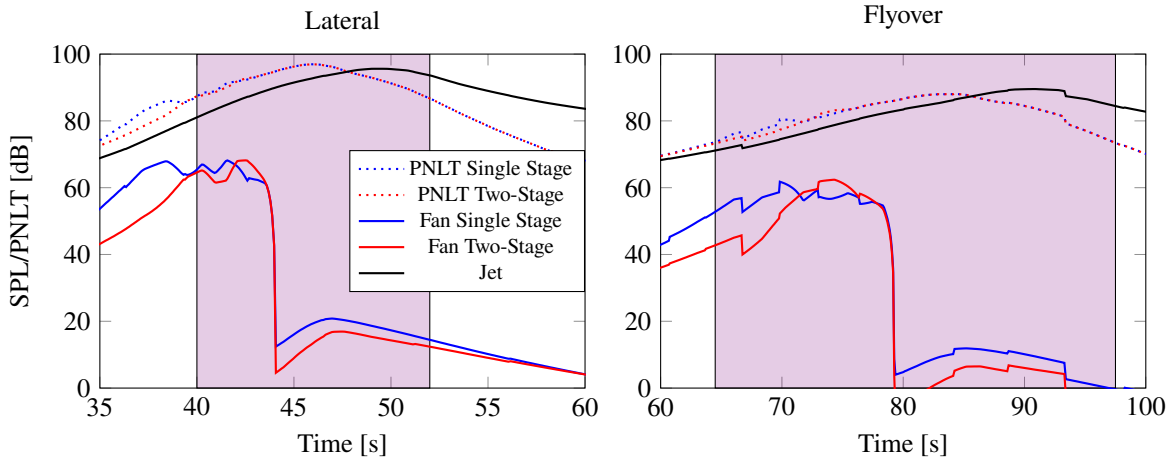

Fig. 8 SPL on baseline trajectory

		Lateral	Flyover	Cumulative
Single Stage	**Limit**	98.2	99.3	285.3
	Noise Levels	94.5	89.1	271.5
	Margins	3.7	10.2	12.8
Two-Stage	**Noise Levels**	94.5	89.0	263.7
	Margins	3.7	10.3	21.6

Table 13 Noise certification levels on the baseline take-off trajectory in EPNdB

C. Take-Off on Optimized Trajectory

For the optimized trajectory, it is important to explore both certification points (Lateral and Flyover) separately, since they have very different operating conditions. Due to the differences in fan noise and thus a different PNLT peak, the position of the Lateral certification point is not the same for both designs. The single stage fan lateral certification point is located 4750m (longitudinal distance) from break release, the two-stage fan's at 3000m from break release. The relevant engine parameters for the Lateral certification points can be found in Table 14. It is easy to see that the thrust setting for these two points is very different.

	Single Stage	**Two-Stage**
Rel. Thrust [%]	51.0	86.0
FPR [−]	1.54	1.83
Jet Mach Number [−]	0.81	0.97
Rel. Fan Speed [%]	80.7	85.7
Rel. Tip Mach Number [−]	1.33	1.11

Table 14 Parameters of optimized take-off Lateral operating points

The time signals of the resulting PNLT, fan and jet noise for each fan's respective Lateral certification point microphone can be seen in Fig.9.

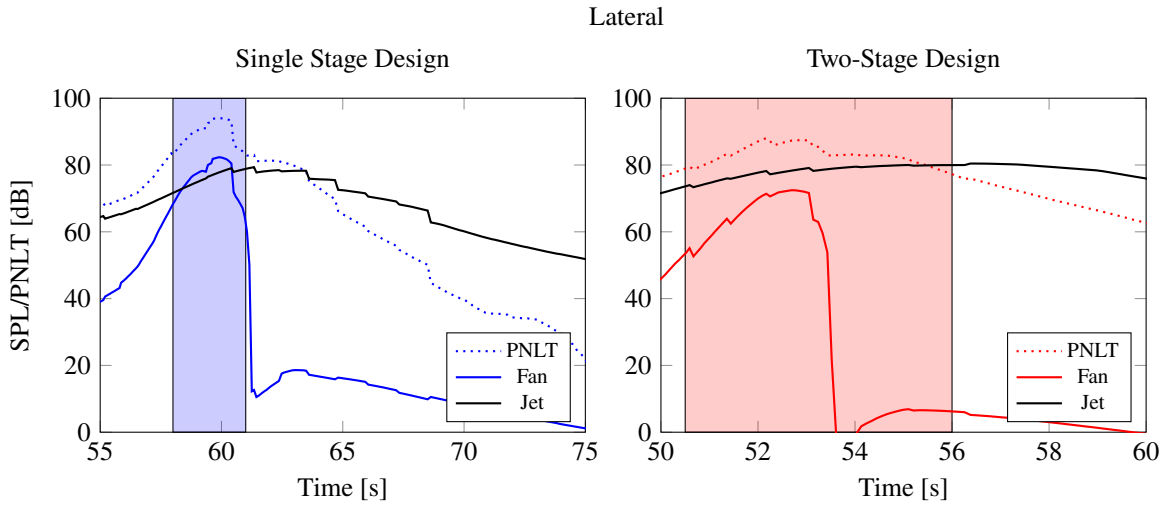

Fig. 9 SPL at Lateral microphones on optimized trajectory, with 10dB down time

The PNLT peak is driven by fan noise for both designs. For the single stage design, fan noise is even dominant over jet noise before frequency weighing and tone correction. As can be seen in Fig.10, the dominant fan noise source for both designs is buzzsaw noise. The stark decrease in fan noise after the fly-by due to liner attenuation can be observed here again. Due to the transonic rotors, inter-stage fan noise sources like rotor-stator interaction noise would in reality not be able to propagate towards the inlet or exhaust plane. They are shielded by the shocks attached to the outer section of the rotor blades, but as mentioned in Section II, transonic rotor shielding is ignored in this study.

Jet noise is the dominant broadband noise source at all times. The higher fan speed and thus relative tip Mach number of the single speed fan (see Table 14) lead to stronger buzzsaw noise than that of the two-stage fan. The main portion of the sound energy in buzzsaw noise being in heavily penalized frequency bands and it being a tonal source increases its impact on certification levels even more.

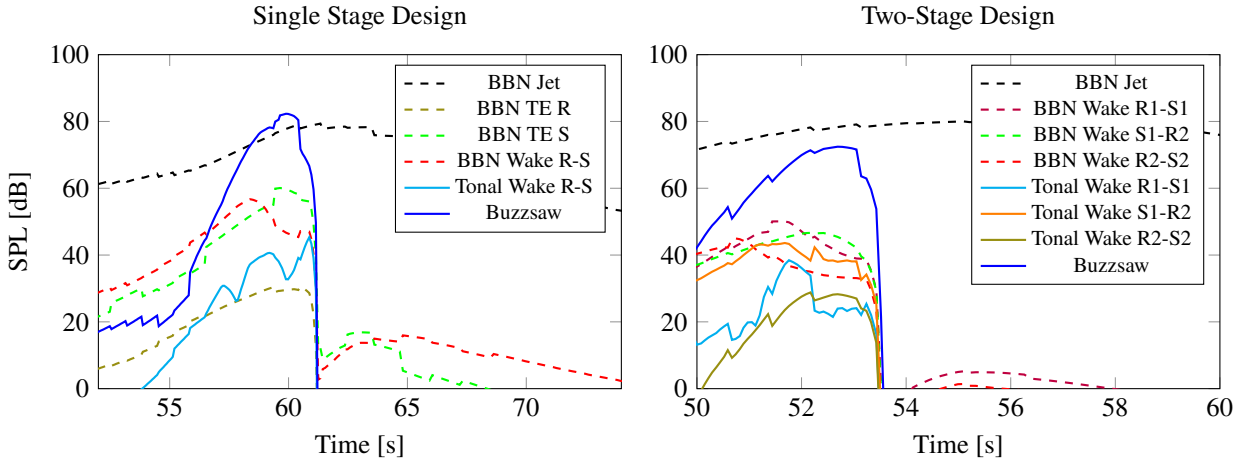

Fig. 10 Individual noise sources at Lateral microphones, broadband sources with dashed and tonal sources with solid plots

At the Flyover certification point, the thrust setting is much lower than on lateral. The representative engine operating conditions are shown in Table 15.

	Single Stage	**Two-Stage**
Rel. Thrust [%]	32.0	
FPR [−]	1.37	
Jet Mach Number [−]	0.69	
Rel. Fan Speed [%]	71.2	72.0
Rel. Tip Mach Number [−]	1.16	0.91

Table 15 Parameters of optimized take-off Flyover operating points

Concerning acoustics, the trend is similar to the Lateral point. Single stage fan noise is dominant over jet noise, dictating PNLT over time, as can be seen in Fig.11. For the two-stage fan, fan noise has a small impact on PNLT, with jet noise being the dominant source.

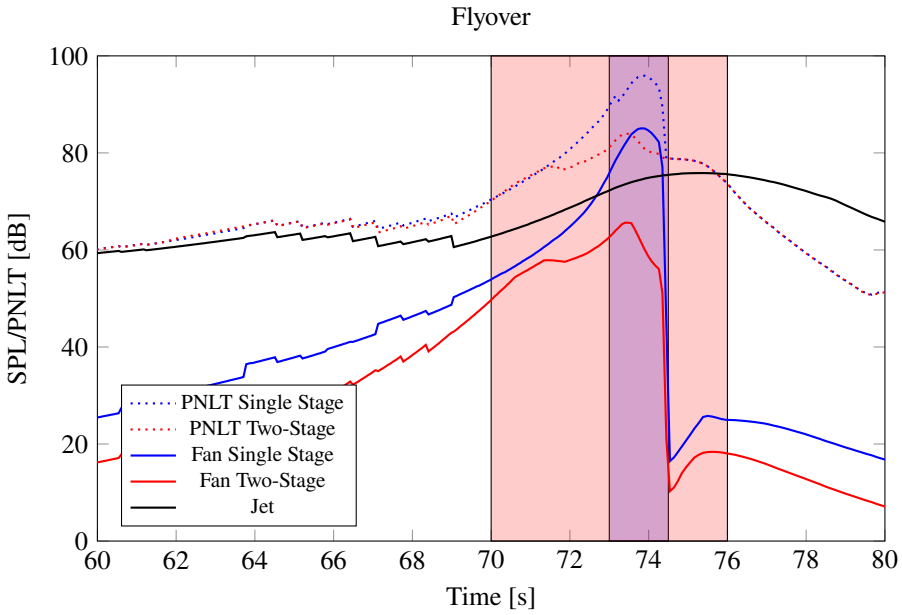

Fig. 11 SPL at Flyover microphone on optimized trajectory, with 10dB down time

The dominant noise source inside the 10 dB down time for the single stage design is buzzsaw noise as illustrated in Fig.12. Jet noise is the dominant broadband noise source at all times. Buzzsaw noise for the two-stage design is non-existent due to the relative tip Mach number of the first stage rotor being below 1 (see Table 15). Its certification noise level at the Flyover point is dominated by jet noise.

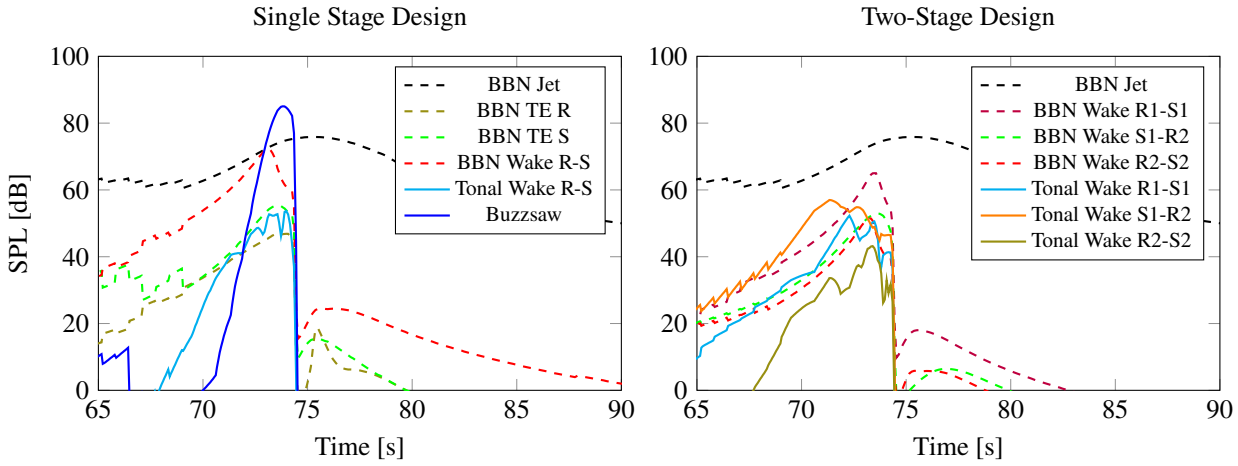

Fig. 12 Individual noise sources at Flyover microphone, broadband sources with dashed and tonal sources with solid plots

The take-off certification noise levels on the optimized trajectory for both fan designs on the optimized trajectory can be seen in Table 16. For this trajectory, there is a clear difference in EPNdB between the two fan designs.

		Lateral	Flyover	Cumulative
Single Stage	**Limit**	98.2	99.3	285.3
	Noise Levels	85.6	85.6	259.1
	Margins	12.6	13.7	26.2
Two-Stage	**Noise Levels**	82.4	76.6	239.2
	Margins	15.8	22.7	46.1

Table 16 Noise certification levels on the optimized take-off trajectory in EPNdB

D. Margins to Chapter 14 Noise Limits

All margins to Chapter 14 noise limits in this study are much higher than expected of a supersonic airliner. Even with the full power take-off on the baseline trajectory, they remain positive. The authors are investigating the reasons for this. There is no definitive explanation as of this writing, but there are several theories:

- Aircraft weight: The airliner with $MTOM \approx 144.3t$ is very light for its mission, compared to a design by Georgia Tech for the ASCENT project ($M_{Cruise} = 1.7$, 65 pax, 4250nm range, $MTOM \approx 199t$) [39]. Empirical models were used in the design and they may not be calibrated for supersonic applications. A lower weight leads to a significantly reduced engine size and thrust demand throughout the entire mission.
- Aerodynamic efficiency: Accurately modelling the low-speed aerodynamics of a delta wing is challenging, so the results need to be scrutinized. An aerodynamic efficiency of up to 11.1 on the baseline and 13.8 on the optimized take-off trajectory appears to be too optimistic. This leads to underestimated thrust demand at low speeds, so all LTO operations. Experimental studies on a delta wing with a similar aspect ratio by Jarrah and Ashley [40] suggest that 8-9 is a more realistic maximum.
- Liner attenuation: With the narrow nacelle of supersonic aircraft engines, the depth of liner cavities is limited, so liner attenuation might be overestimated. Furthermore, the boundary layer and inflow distortion present at the high angle of attack at low speeds deteriorate the liner performance, which was not accounted for in this study.

VII. Conclusion

In this study, the authors are able to show that there are significant differences between the operation of a single and a two-stage fan for supersonic aircraft in LTO conditions. In general, a two-stage fan can produce the required FPR at much lower speeds and with shorter blade chords. This leads to lower fan noise and depending on the engine's operation, can impact the aircraft's certification noise levels.

At high power settings, the broadband jet noise is the dominant source and the difference in fan noise contribution to noise certification levels between single stage and two-stage designs is not relevant. It is however unlikely that Chapter 14 levels can be met without the use of VNRS and the resulting lower power settings.

Lower thrust settings that are achieved on approach or by the use of VNRS on take-off can make fan noise a dominant source. In these cases, the two-stage fan yields a significant advantage through two main mechanisms:

- Fan tip speed: On medium power settings, its lower fan speeds keep the relative tip Mach number below 1 and thus eliminate buzzsaw noise. The same is not true for the faster single stage fan, where buzzsaw noise is the dominant noise source.
- Narrower rotor chords: On low power settings, both fans operate with high rotor incidences which lead to strong, turbulent wakes. The smaller chord length of the two-stage fan leads to smaller, less turbulent wakes and thus significantly lower broadband rotor-stator interaction noise.

The two-stage design has disadvantages such as increased weight, space needs and complexity. However the exploration of these is not within the scope of this paper.

Since some simplifications were made for this study, there are ways in which to improve the quality of the absolute certification noise levels:

- Adding a more sophisticated and accurate liner model to more accurately predict the spectrum of the fan noise radiated from inlet and nozzle. Different attenuation depending on frequency can impact the source ranking as well as the overall fan noise and significantly alter the resulting PNLT and thus EPNL. The liner efficiency depending on the fan speed can also be modelled much more accurately.

- Including shielding effects, since fan noise can be attenuated by wing shielding in engine-over-wing configurations and reflected in underwing configurations, while jet noise is not usually shielded or reflected in a relevant capacity. This could lead to fan noise being dominant where jet noise was found to be dominant in this paper and vice-versa.
- Including transmission effects to more accurately predict the propagation of inter-stage noise sources for the two-stage design. The transonic rotor shielding could effectively eliminate inter-stage noise sources and reduce the radiated noise. This is particularly true for the two-stage design, since both rotors can shield up- and downstream sources.

Acknowledgments

The authors thank the European Union for the financial support in the context of the Horizon 2020 Research and Innovation Programme (Project SENECA, Grant Agreement No. 101006742).

References

[1] Scanlan, A., "Boom Supersonic Begins Construction on Overture Superfactory," , 2023. URL https://boom-press-assets.s3.us-west-2.amazonaws.com/Boom_Supersonic_Groundbreaking.pdf.

[2] Munoz, C. V., Bonavolontà, G., Lawson, C., and Riaz, A., "Conceptual Design of a Next Generation Supersonic Airliner for Low Noise and Emissions," *AIAA SCITECH 2023 Forum*, American Institute of Aeronautics and Astronautics, Reston, Virigina, 2023. https://doi.org/10.2514/6.2023-0215.

[3] Villena Munoz, C., Lawson, C., Riaz, A., and Sharma, A., "Design of the SENECA Mach 1.8 Supersonic Airliner with Multi-Fidelity Aerodynamic Analysis for Noise-Optimized Take-Off Trajectories," *34th ICAS PROCEEDINGS*, The International Council of the Aeronautical Sciences, Florence, Italy, 2024. URL https://www.icas.org/ICAS_ARCHIVE/ICAS2024/data/papers/ICAS2024_0758_paper.pdf.

[4] Plohr, M., Zenkner, S., Bake, S., and Zeitz, D., "Thermodynamic Design and Emissions Model of a Mach 1.8 Supersonic Airliner Engine," *34th ICAS PROCEEDINGS*, The International Council of the Aeronautical Sciences, Florence, Italy, 2024. URL https://www.icas.org/ICAS_ARCHIVE/ICAS2024/data/papers/ICAS2024_0129_paper.pdf.

[5] Heidmann, M. F., "Interim prediction method for fan and compressor source noise," Technical Memorandum X-71763, NASA, Cincinnati, OH, Jun. 1979.

[6] Kontos, K. B., Kraft, R. E., and Gliebe, P. R., "Improved NASA-ANOPP noise prediction computer code for advanced subsonic propulsion systems," Contractor Report CR-202309, General Electric Co., Cincinnati, OH, Dec. 1996.

[7] Kresja, E. A., and Stone, J. R., "Enhanced Fan Noise Modeling for Turbofan Engines," , Dec. 2014. URL https://ntrs.nasa.gov/api/citations/20150000884/downloads/20150000884.pdf.

[8] Gliebe, P., "XF-120 Fan Noise Correlation," Memorandum C1-1L5-FP-96-149, GE Aircraft Engines, 1996.

[9] Rawls Jr., J. W., and Yeager, J. C., *High Speed Research Noise Prediction Code(HSRNOISE) User's and Theoretical Manual*, Lockheed Martin Engineering and Sciences Company, Hampton, VA, 2004. URL https://ntrs.nasa.gov/api/citations/20040200978/downloads/20040200978.pdf.

[10] Berton, J. J., "Aircraft Noise and Performance Data for a Notional Supersonic Business Jet," *28th AIAA/CEAS Aeroacoustics 2022 Conference*, American Institute of Aeronautics and Astronautics, Reston, Virigina, 2022. https://doi.org/10.2514/6.2022-3078.

[11] Nöding, M., Schuermann, M., Bertsch, L., Koch, M., Plohr, M., Jaron, R., and Berton, J. J., "Simulation of Landing and Take-Off Noise for Supersonic Transport Aircraft at a Conceptual Design Fidelity Level," *Aerospace*, Vol. 9, No. 1, 2022, p. 9. https://doi.org/10.3390/aerospace9010009.

[12] Nöding, M., Bertsch, L., Kirz, J., Ewert, R., and Berton, J. J., "Application and comparison of proposed SST noise certification regulations to a conceptual business aircraft," *AIAA AVIATION 2023 Forum*, American Institute of Aeronautics and Astronautics, 2023. https://doi.org/10.2514/6.2023-4169.

[13] Akatsuka, J., and Ishii, T., "System Noise Assessment and Uncertainty Analysis of a Conceptual Supersonic Aircraft," *Aerospace*, Vol. 9, No. 4, 2022, p. 212. https://doi.org/10.3390/aerospace9040212.

[14] Stephens, D., "Fan Noise for a Concept Commercial Supersonic Transport," *53rd AIAA/SAE/ASEE Joint Propulsion Conference*, American Institute of Aeronautics and Astronautics, Reston, VA, 2017. https://doi.org/10.2514/6.2017-4635.

[15] Stephens, D., "Acoustic Simulations and Commercial Supersonic Flight," , October 2021. URL https://ntrs.nasa.gov/api/citations/20210021219/downloads/Stephens_NASA_Acoustic%20Simulations%20and%20Commercial%20Supersonics.pdf.

[16] Moreau, S., "A Review of Turbomachinery Noise: From Analytical Models to High-Fidelity Simulations," *Fundamentals of High Lift for Future Civil Aircraft*, Notes on Numerical Fluid Mechanics and Multidisciplinary Design, Vol. 145, edited by R. Radespiel and R. Semaan, Springer International Publishing, Cham, 2021, pp. 579–595. https://doi.org/10.1007/978-3-030-52429-6_35.

[17] Graebert, M., Jaron, R., Plohr, M., Zenkner, S., Richter, C., Stöhr, C., Munoz, C. V., van der Meulen, M.-J., Habing, R., Huet, M., Petrosino, F., Barbarino, M., Fischer, F., and Zaporozhets, O., "Landing and Take-Off Noise Prediction of Conceptual Supersonic Aircraft," *34th ICAS PROCEEDINGS*, The International Council of the Aeronautical Sciences, Florence, Italy, 2024. URL https://www.icas.org/ICAS_ARCHIVE/ICAS2024/data/papers/ICAS2024_0121_paper.pdf.

[18] Moreau, S., "Turbomachinery Noise Predictions: Present and Future," *Acoustics*, Vol. 1, No. 1, 2019, pp. 92–116. https://doi.org/10.3390/acoustics1010008.

[19] Messenger, H. E., and Kennedy, E., "Two-Stage Fan I: Aerodynamic and Mechanical Design," Contractor Report CR-120859, Pratt and Whitney Aircraft, East Hartford, CT, Jan. 1972. URL https://ntrs.nasa.gov/api/citations/19720013113/downloads/19720013113.pdf.

[20] Ruggeri, R. S., and Benser, W. A., "Performance of a highly loaded two stage axial-flow fan," Technical Memorandum TM X-3076, NASA Lewis Research Center, Cleveland, OH, Aug. 1974. URL https://ntrs.nasa.gov/api/citations/19740023305/downloads/19740023305.pdf.

[21] Cunnan, W. S., Stevens, W., and Urasek, D. C., "Design and performance of a 427-meter-per-second-tip-speed two-stage fan having a 2.40 pressure ratio," NASA technical paper 1314, NASA Lewis Research Center, Cleveland, OH, 1978. URL https://ntrs.nasa.gov/api/citations/19780025166/downloads/19780025166.pdf.

[22] Antl, R. J., "The effect of noise constraints on engine cycle optimization for long-haul transports," *9th Propulsion Conference*, American Institute of Aeronautics and Astronautics, Reston, Virigina, 1973. https://doi.org/10.2514/6.1973-1292.

[23] Calvert, W. J., and Ginder, R. B., "Transonic fan and compressor design," *Proceedings of the Institution of Mechanical Engineers, Part C: Journal of Mechanical Engineering Science*, Vol. 213, No. 5, 1999, pp. 419–436. https://doi.org/10.1243/0954406991522671.

[24] Moreau, A., "A unified analytical approach for the acoustic conceptual design of fans of modern aero-engines," Ph.D. thesis, TU-Berlin, 2017.

[25] Moreau, A., Staggat, M., and Gscheidle, C., "A Fast Prediction Method for Rotor Buzz-saw Noise based on an Analytical Approach," *25th AIAA/CEAS Aeroacoustics Conference*, American Institute of Aeronautics and Astronautics, Reston, VA, 2019. https://doi.org/10.2514/6.2019-2641.

[26] Stone, J. R., Groesbeck, D. E., and Zola, C. L., "Conventional profile coaxial jet noise prediction," *AIAA Journal*, Vol. 21, No. 3, 1983, pp. 336–342. https://doi.org/10.2514/3.8077.

[27] Moreau, A., Prescher, A., Schade, S., Dang, M., Jaron, R., and Guérin, S., "A framework to simulate and to auralize the sound emitted by aircraft engines," *2023 InterNoise Conference*, Chiba, Japan, 2023.

[28] International Organization for Standardization, "Acoustics - Attenuation of sound during propagation outdoors: Part 1: Calculation of the absorption of sound by the atmosphere," , Jun. 1993. URL https://cdn.standards.iteh.ai/samples/17426/3a2d69b767024b74805b83b063a91445/ISO-9613-1-1993.pdf.

[29] *Method for Predicting Lateral Attenuation of Airplane Noise*, SAE, Warrendale, Pennsylvania, Oct. 2019. https://doi.org/10.4271/air5662.

[30] Prescher, A., "Modellierung der Schallausbreitung in einer inhomogenen Atmosphäre und ihr Einfluss auf binaural synthetisierten Überfluglärm," Master's thesis, TU Berlin, Berlin, 2023.

[31] Rice, E. J., "Propagation of Waves in an Acoustically Lined Duct with a Mean Flow," *Basic Aerodynamic Noise Research: A Conference Held at NASA Headquarters, Washington, DC, July 14-15, 1969*, Vol. 207, Scientific and Technical Information Division, National Aeronautics and . . . , 1969, p. 345.

[32] Rice, E., "Acoustic liner optimum impedance for spinning modes with mode cut-off ratio as the design criterion," *3rd Aeroacoustics Conference*, American Institute of Aeronautics and Astronautics, 1976. https://doi.org/10.2514/6.1976-516.

[33] Rice, E. J., "Inlet noise suppressor design method based upon the distribution of acoustic power with mode cutoff ratio," *Advan. in Eng. Sci., Vol. 3*, 1976. URL https://ntrs.nasa.gov/api/citations/19770003369/downloads/19770003369.pdf.

[34] Rice, E. J., and Sawdy, D. T., "A theoretical approach to sound propagation and radiation for ducts with suppressors," *Meeting of the ASA*, 1981. URL https://ntrs.nasa.gov/api/citations/19810014304/downloads/19810014304.pdf.

[35] Rienstra, S., "Impedance models in time domain, including the extended Helmholtz resonator model," *12th AIAA/CEAS Aeroacoustics Conference (27th AIAA Aeroacoustics Conference)*, 2006, p. 2686. https://doi.org/https://doi.org/10.2514/6.2006-2686.

[36] Graebert, M., Jaron, R., Moreau, A., and Plohr, M., "Aeroakustischer Vergleich eines ein- und eines mehrstufigen Fan-Konzepts für zivile überschallfähige Triebwerke," 2023. https://doi.org/10.25967/610277.

[37] Miller, G. R., Lewis, G. W., and Hartmann, M. J., "Shock Losses in Transonic Compressor Blade Rows," *Journal of Engineering for Power*, Vol. 83, No. 3, 1961, pp. 235–241. https://doi.org/10.1115/1.3673182.

[38] ICAO, "Annex 16 - Environmental Protection - Vol.I," International Standards and Recommended Practices 8, International Civil Aviation Organization, Montréal, Canada, 2017.

[39] Mavris, D., Tai, J., Crossley, W. A., and D., D., "ASCENT Project 010 2023 Annual Report," Tech. rep., Georgia Institute of Technology, Purdue University, 2023. URL https://s3.wp.wsu.edu/uploads/sites/2479/2024/05/ASCENT-Project-010-2023-Annual-Report.pdf.

[40] Jarrah, M., and Ashley, H., "Impact of flow unsteadiness on maneuvers and loads of agile aircraft," *30th Structures, Structural Dynamics and Materials Conference*, American Institute of Aeronautics and Astronautics, 1989. https://doi.org/10.2514/6.1989-1282.

Appendix

		Approach		Lateral Baseline	Flyover Baseline	Cum. Baseline		Lateral Opt.	Flyover Opt.	Cum. Opt.
Single Stage	**Noise Levels**	102.7		107.2	101.0	310.9		111.9	113.1	327.7
	Margins	-0.9		-9.0	-1.7	-25.6		-13.7	-13.8	-42.5
Two-Stage	**Noise Levels**	101.9		104.9	99.4	306.2		102.5	98.7	303.1
	Margins	-0.1		-6.7	-0.1	-20.9		-4.3	0.6	-17.8

Table 17 Noise certification levels without liners in EPNdB

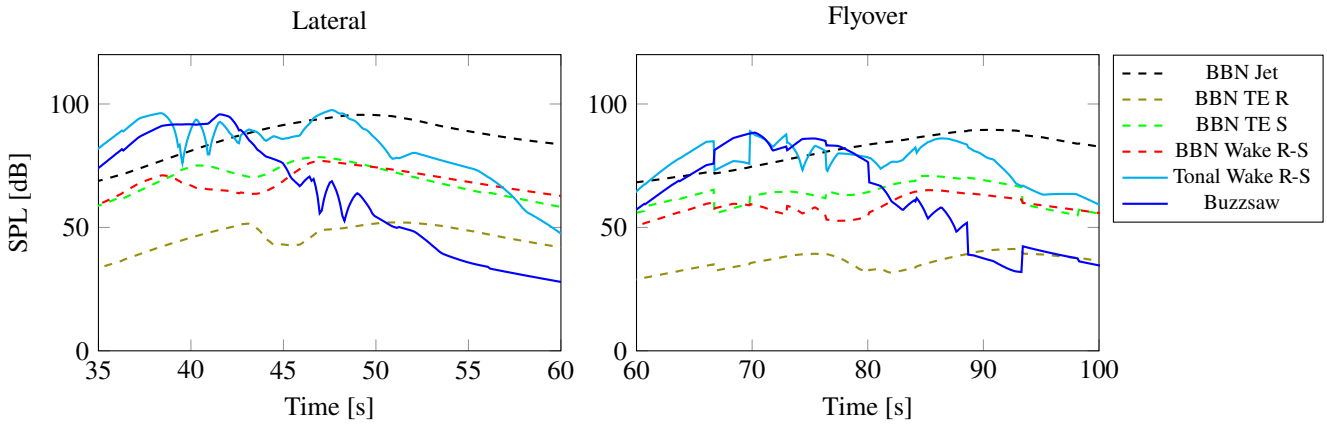

Fig. 13 Single stage design - baseline take-off without liners

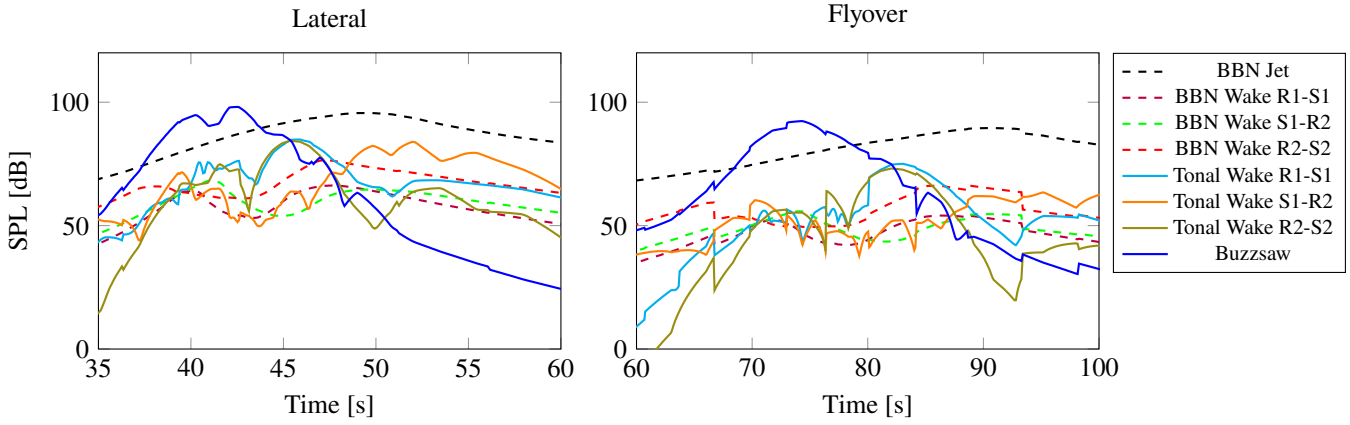

Fig. 14 Two-stage design - baseline take-off without liners

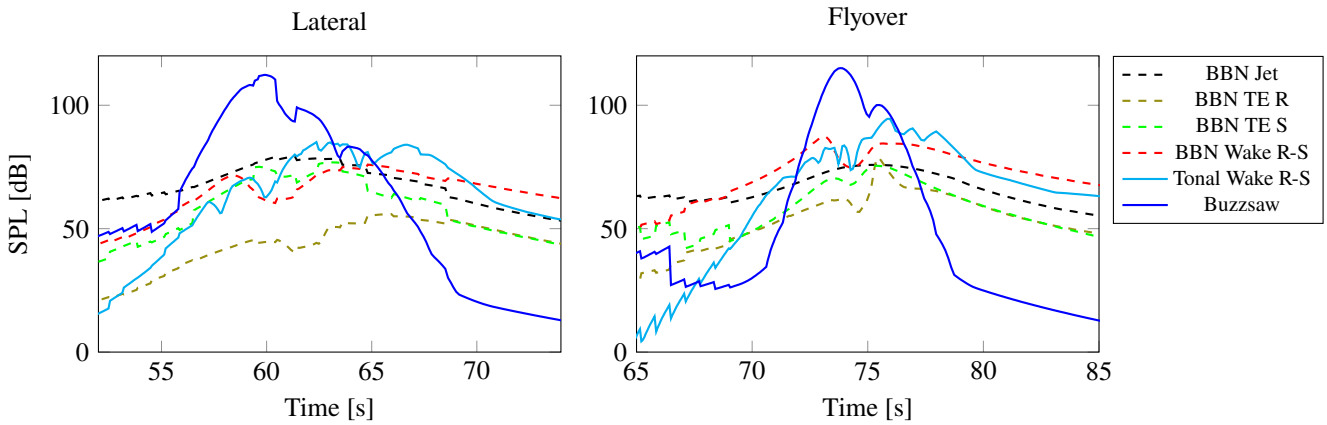

Fig. 15 Single stage design - optimized take-off without liners

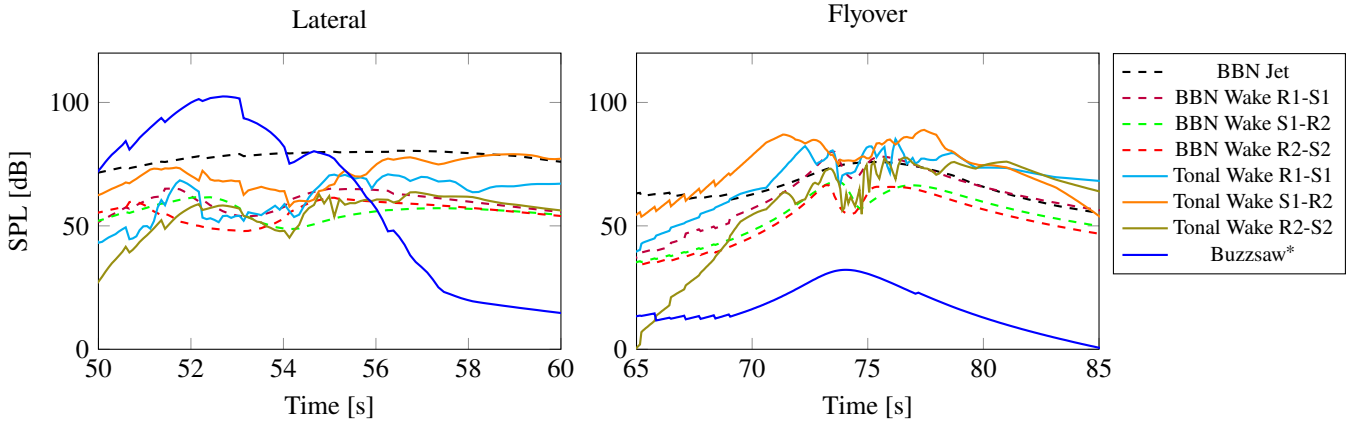

Fig. 16 Two-stage design - optimized take-off without liners

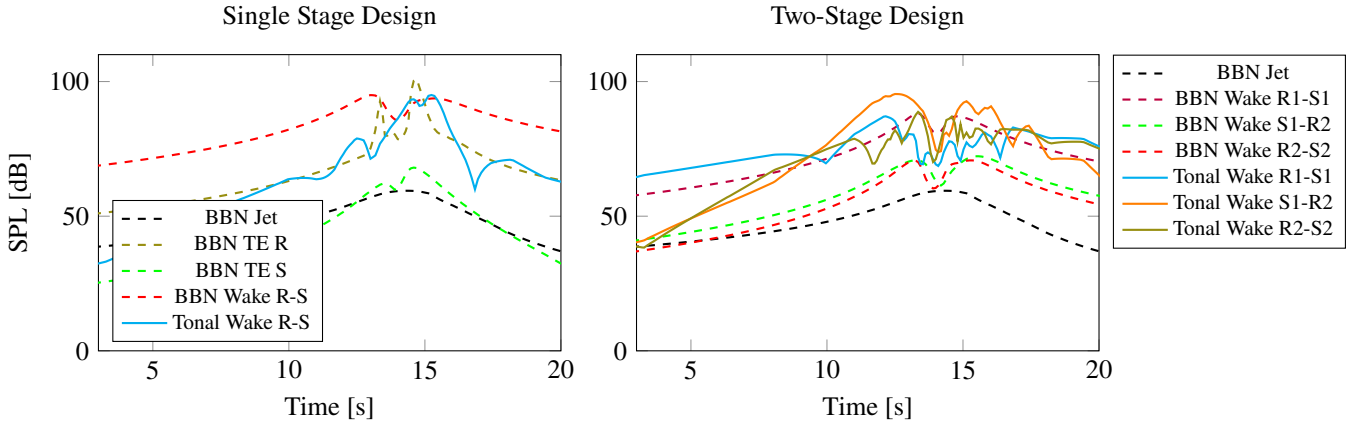

Fig. 17 Both designs - Approach without liners

*In Flyover operation, the potential field of the subsonic rotor is a noise source similar to buzzsaw and is labeled as such for simplicity

https://dspace.org/

Single- and two-stage fan designs for a supersonic airliner with focus on certification noise reduction

Graebert, Matti; Jaron, Robert; Villena Munoz, Cristina; Plohr, Martin; Moreau, Antoine

2025-01-06
American Institute of Aeronautics and Astronautics (AIAA)
https://doi.org/10.2514/6.2025-2680
Graebert M, Jaron R, Villena Munoz C, et al., (2025) Single- and two-stage fan designs for a supersonic airliner with focus on certification noise reduction. In: AIAA SCITECH 2025 Forum, 6-10 January 2025, Orlando, FL, USA. Paper number AIAA 2025-2680

Downloaded from a DSpace repository. https://dspace.org/